

Preparation and Characterization of Sulfonated Poly(phthalazinone ether sulfone ketone) (SPPEsk)/Silica Hybrid Membranes for Direct Methanol Fuel Cell Applications

Dae Sik Kim, Kwang Ho Shin, Ho Bum Park and Young Moo Lee*

National Research Laboratory for Membranes, School of Chemical Engineering,
College of Engineering, Hanyang University, Seoul 133-791, Korea

Received May 7, 2004; Revised June 23, 2004

Abstract: Sulfonated poly(phthalazinone ether sulfone ketone) (SPPEsk) membranes and sol-gel derived SPPEsk/silica hybrid membranes have been investigated as potential polymer electrolyte membranes for direct methanol fuel cell (DMFC) applications. In comparison with the SPPEsk membrane, the SPPEsk/silica membranes exhibited higher water content, improved proton conductivity, and lower methanol permeability. Notably, the silica embedded in the membrane acted as a material for reducing the fraction of free water and as a barrier for methanol transport through the membrane. From the results of proton conductivity and methanol permeability studies, we suggest that the fractions of bound and free water should be optimized to obtain desirable proton conductivities and methanol permeabilities. The highly sulfonated PPEsk hybrid membrane (HSP-Si) displayed higher proton conductivity (3.42×10^2 S/cm) and lower methanol permeability (4.15×10^7 cm²/s) than those of Nafion 117 (2.54×10^2 S/cm; 2.36×10^6 cm²/s, respectively) at 30 °C. This characteristic of the SPPEsk/silica membranes is desirable for future applications related to DMFCs.

Keywords: sulfonated poly(phthalazinone ether sulfone ketone) (SPPEsk), silica, proton conductivity, methanol permeability, hybrid membrane.

Introduction

A direct methanol fuel cells (DMFCs) using polymer electrolyte membranes has gained much interest as a candidate for the application of portable power source and transport application because they do not require any fuel processing equipment such as reformer and catalytic burner.¹⁻³ Nafion, a fluorinated ionomer, has been commonly used for fuel cell applications. It shows high proton conductivity and chemical stability, but the methanol permeability is too high, which makes Nafion difficult for DMFC application.⁴ For use in fuel cell, the following properties of polymer electrolyte membranes need to be optimized: (1) high proton conductivity, (2) good mechanical, chemical and thermal strength, (3) low gas permeability, and (4) low electro-osmotic drag coefficient to reduce methanol crossover for DMFC applications.⁵

Considerable efforts have been developed in order to reduce methanol permeability as well as to reach high proton conductivity. For instance, membranes containing metallic

blocking layers have been proposed.⁶ Organic-inorganic composite membranes containing Zr-phosphonates, tin doped mordenites, zeolites or silica were investigated.⁷⁻¹⁰ Mauritz *et al.*¹¹ have reported a Nafion/silica hybrid membrane using sol-gel reaction of tetraethoxysilane (TEOS) to form silica inside the Nafion membrane.

Various sulfonation techniques are commonly applied to modify polymers to increase hydrophilicity and ionic character.¹²⁻¹⁵ Typical methods include the sulfonation on pendant aromatic rings of fluorinated polymer¹⁶ or direct sulfonation on the backbone of aromatic polymers.¹⁷ For example, sulfonated polysulfones and polyetherketones have been reported to be useful in desalination, ion exchange and fuel cell membrane applications.¹⁸⁻²⁰

Particularly poly(phthalazinone ether sulfone ketone) (PPEsk) has high glass transition temperature and excellent mechanical property and thermal stability. It was reported that the membranes made from PPEsk showed good separation and permeation properties for gas and liquid separation.²¹ Yan *et al.*²² reported that sulfonated poly(phthalazinone ether sulfone)s were prepared to improve the hydrophilicity and thereby to use as polymer electrolyte membrane. Recently, the sulfonation and synthesis methods of poly

*e-mail: ymlee@hanyang.ac.kr

1598-5032/08/413-09©2004 Polymer Society of Korea

(phthalazinone arylene ether)s have been reported for proton exchange membrane materials and these membrane shows high proton conductivity of up to $\sim 10^{-2}$ S/cm.²³⁻²⁵ However, the methanol transport behavior of these membranes was not reported.

The objective of this study is to prepare sulfonated PPESK and confirm that the hydrolysis of the TEOS added to the sulfonated PPESK polymer solution led to the formation of a common network providing a good adhesion between organic and inorganic phases. To achieve this objective, the introduction of sulfonic acid group into PPESK polymer matrix was achieved by the sulfonation with a concentrated sulfuric acid or a fuming sulfuric acid under various conditions. Silica was introduced into the polymer matrix using sol-gel reaction under acidic conditions, which was expected to provide a barrier to methanol transport. Here, the state of water, ion exchange capacity, proton conductivity and methanol permeability in the SPPEK/silica membrane were investigated to characterize membranes for DMFC application.

Experimental

Materials. PPESK random copolymer ($M_w = 39,000$, Polymer New Material Co., Ltd. Dalian, China) used in this study had a sulfone/ketone ratio of 1 : 1. Tetraethyl orthosilicate (TEOS) and methanol (MeOH) were analytical grade from Aldrich Chemical Co., Milwaukee, WI, USA. *N*-methyl-2-pyrrolidinone (NMP), concentrated (98%) sulfuric acid, fuming sulfuric acid (20-25% SO_3), and other chemicals used were also purchased from Aldrich, and were of analytical grade.

Membrane Preparation. PPESK powders were completely dried in a vacuum oven at 120°C for 24 h before use. The PPESK and the concentrated sulfuric acid were placed in a three-neck reaction vessel equipped with a mechanical stirrer. The sulfonated PPESKs (SPPEK) with different degrees of sulfonation were obtained at 60°C reaction temperature, and the sulfonation level was controlled by various reaction time from 6 to 50 h. Hereafter we denoted samples as SP-XX, where XX refers to sulfonation time. The sulfonated polymers were precipitated in ethanol and then filtered. The polymers were washed several times with ethanol/water to remove acid until pH was neutral. All the polymers were filtered and then dried in a vacuum oven at 120°C for 24 h. In a highly sulfonated PPESK (denoted as HSP), PPESK powder was added to a mixture of H_2SO_4 /fuming SO_3 (4 : 6 v/v) under an N_2 gas at temperature 60°C for 4 h. The sulfonated polymers were poured onto crushed ice. The HSP polymer isolation steps were similar to those previously described for SP-XX.

The sulfonated PPESK membrane was obtained by a solution casting method. The sulfonated polymer (10 wt%) was dissolved in NMP. The sulfonated polymer solution

was poured into a glass plate and cast using a casting knife.

SPPEK/silica hybrid membranes were prepared by dissolving the sulfonated PPESK in NMP followed by addition of TEOS solution, which was prepared by mixing $\text{H}_2\text{O}/\text{HCl}/\text{TEOS}$ in a mole ratio of 4/0.1/1. The TEOS solution was added as 5% by weight to polymer weight. The solution was mixed for 12 h at room temperature under a N_2 atmosphere. The SPPEK and silica sol solution were poured into a glass plate. All the cast membranes were initially heated at 80°C for 24 h, then 100°C for 24 h (hereafter, denoted as SP-Si-XX and HSP-Si, where XX refers to sulfonation time).

Membrane Characterization. The FT-IR spectra were measured using a Nicolet IR 860 spectrometer (Nicolet Model Magna IR 550, Madison, WI, USA) in the wavenumber range between 4000-500 cm^{-1} .

To study the morphology of membranes, the surfaces were investigated using field emission scanning electron microscope (FE-SEM, Jeol Model JSF 6340F, Tokyo, Japan). $^1\text{H-NMR}$ spectra were recorded using a NMR spectrometer (Varian model NMR 1000 spectrometer, Varian Inc., Palo Alto, CA, USA.) $^1\text{H-NMR}$ spectra of PPESK in CDCl_3 and SPPEK in DMSO-d_6 were recorded.

The thermal degradation behavior of all the membranes was studied using a thermogravimetric analysis (TGA 2050, TA Instrument, New Castle, DE, USA). The TGA measurement was carried out under the nitrogen atmosphere at a heating rate of 10°C/min from 50 to 700°C.

Differential scanning calorimeter (DSC) measurement was carried out using a DSC 2010 thermal analyzer (TA Instrument, New Castle, DE, USA) equipped with a cooling apparatus. After cooling with liquid nitrogen, the experiment was started by heating from -50 to 50°C at a rate of 5°C/min under a nitrogen purge flow.

Water Vapor Sorption and IEC. Water vapor sorption experiment was performed using a dynamic vapor sorption apparatus (DVS-1000, Surface Measurement Systems Ltd, London, UK) at RH 3090%.

The water content was measured as follows. After soaking the samples in distilled water for two days, they were wiped with filter paper and weighed immediately. The water content (%) was determined by:

$$\text{Water content (\%)} = (W_{\text{wet}} - W_{\text{dry}}) / W_{\text{dry}} \times 100 \quad (1)$$

where W_{wet} and W_{dry} are the wet and dried membrane weight, respectively.

Ion-exchange capacity (IEC) was determined using the classical titration method. The membranes were protonated in 0.1 M HCl solution for 24 h. The membranes were washed thoroughly with water until pH neutral and then immersed into 0.01 M NaCl solution to replace H^+ by Na^+ -form. The remaining liquid was titrated with 0.01 M NaOH solution using phenolphthalein as an indicator. The unit of IEC was expressed as meq.(- SO_3H)/g dry polymer.

To confirm the stability of membrane in hydrolytic condition, the membranes were immersed in boiling water for two weeks. The IEC value of the membrane was measured after boiling water test.

Proton Conductivity and Methanol Permeability. The proton conductivity in the SPPEESK membranes was measured using a four-point probe technique. The impedance of membrane was determined using Full Material Impedance System 12608 W consisted of a Frequency Response Analyzer 1260 and Electrochemical Interface 1287 (Solatron analytical, Berks, UK). The impedance analyzer was worked in galvanostatic mode with ac current amplitude of 0.1 mA over frequency range from 100 KHz to 0.1 Hz by Nyquist method. The hydrated sample with deionized water for 24 h was cut in $(4 \times 1) \text{ cm}^2$ prior to being mounted on the cell. The impedance of membrane was taken at zero imaginary impedance. The impedance of each sample was measured five times to ensure good data reproducibility. The proton conductivity (σ) was obtained using the following equation:

$$\sigma = \frac{L}{R \cdot S} \quad (2)$$

where σ is proton conductivity (in S/cm). L is the distance between the electrodes to measure the potential (in 1 cm). R is the impedance of membrane (in Ω). S is surface area for proton to penetrate through (in cm^2). The impedance of each sample was measured five times to ensure good data reproducibility.

The methanol permeability of the membranes was determined using a glass diffusion cell.²⁶ This cell consisted of two reservoirs each approximately 80 mL, separated by a vertical membrane. Prior to the test, the membranes were equilibrated in distilled water for at least 12 h. Initially, one reservoir (V_A) contained a 2 M methanol-water solution, and the other reservoir (V_B) contained only pure ionized water. The increase in concentration of methanol in water reservoir was measured across time using a gas chromatography. In the gas chromatography measurements, $1 \mu\text{L}$ samples were analyzed using a Shimadzu GC-14B gas chromatograph (Shimadzu Co. Kyoto, Japan). During the permeability tests, the temperature was controlled by means of a thermostatic water bath. Finally, Methanol permeability was obtained by analyzing the methanol flux with time. The methanol concentration in the V_B reservoir as a function of time is given by

$$C_B(t) = \frac{A DK}{V_B L} C_A(t-t_0) \quad (3)$$

$$P = DK = \frac{1}{A} \frac{C_B(t)}{C_A(t-t_0)} V_B L \quad (4)$$

where C_B and C_A are the two methanol concentration, A and L are the membrane area and thickness, and D and K are

the methanol diffusivity and partition coefficient between the membrane and the adjacent solution, respectively. The assumptions made in this study were that the value of D inside the membrane is constant, and that the value of K did not depend upon the methanol concentration. The product, DK , denotes the membrane permeability ($P(\text{cm}^2/\text{s})$). The value of C_B was measured several times during the experiments, and the permeability was calculated from the gradient of the straight lines obtained from plots of the data.

Results and Discussion

IR Spectra. The FT-IR spectra of the PPESK and the SPPEESK/silica hybrid membranes are shown in Figure 1. The FT-IR spectra showed an absorption band at 1666 cm^{-1} , due to the Ar-C=O stretching, an absorption band of aromatic C=C stretching at 1591 cm^{-1} and C-O-C stretching vibration peak at 1240 cm^{-1} .²⁷ The IR spectra of the SPPEESK/silica hybrid membrane showed a strong absorption at 1025 cm^{-1} (sym. O=S=O stretching of the sulfonated group),

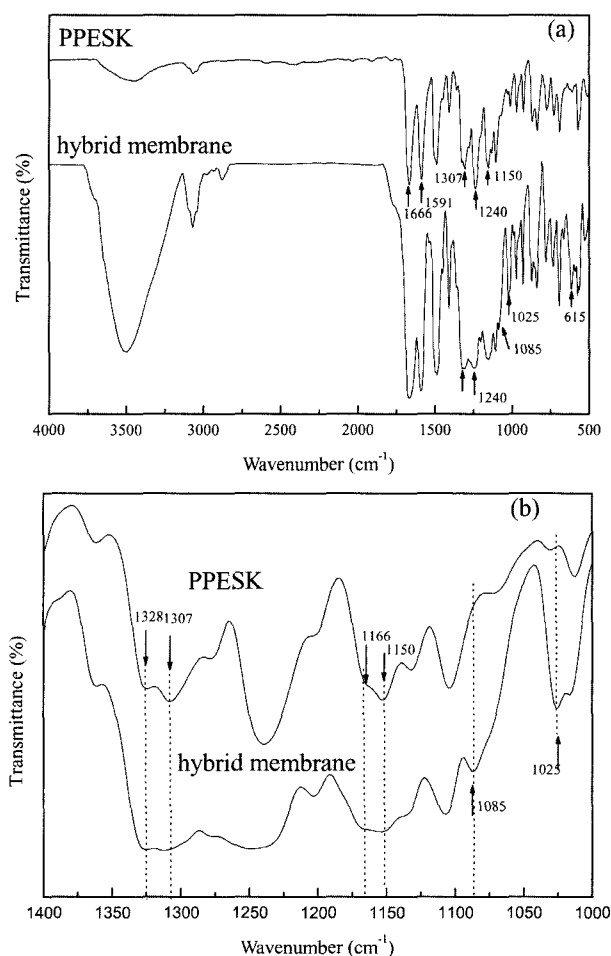


Figure 1. FT-IR spectra of the PPESK and the sulfonated hybrid membrane (SP-Si 50).

and also at 615 cm^{-1} (C-S bond). In addition, the FT-IR spectra of the SPPEK/silica hybrid membrane showed the broad sulfone asymmetric and symmetric absorption bands at $1328\text{--}1307$ and $1150\text{--}1160\text{ cm}^{-1}$. As shown in Figure 1(b), in the spectra of SPPEK/silica hybrid membrane, a new absorption peak appears at 1085 cm^{-1} , which is not observed in the PPESK membrane. This is a characteristic peak of the aromatic SO_3H asymmetric stretching vibration. Therefore, it is clear that the spectral changes are the evidence of sulfonation reaction. As shown in Figure 1(a), the broad band at around $1085\text{--}1220\text{ cm}^{-1}$ (Si-O-Si asymmetric stretching) is seen in the spectra of the SPPEK/silica hybrid membrane. The absorption in the $3700\text{--}3200\text{ cm}^{-1}$ is characterized by silanol groups (Si-OH) formed during the hydrolysis of alkoxy group in TEOS. This indicates that the hybrid membrane was made through the acid-catalyzed sol-gel reaction of TEOS to form silica inside the SPPEK membrane. Deng *et al.*²⁸ reported that the introduction of silica enhanced the hydrophilicity in Nafion owing to the presence of numerous =SiOH group and suggested that the physically sorbed water should be driven off at a higher temperature, around 170°C , as compared with H_2O in $-\text{SO}_3\text{H}\text{--}\text{H}_2\text{O}$ bonds.^{28,29} We expect that the silica particles retain water even at high temperatures and this property may help to prevent the drying of the membrane during the measurement of proton conductivity.

NMR Spectrum. ^1H -NMR spectra of PPESK in CDCl_3 and sulfonated PPESK in $\text{DMSO-}d_6$ were characterized. The spectrum of PPESK shown in Figure 2(a) is broadly divided into three groups of multiplets: H-8 (S or K unit) at low field ($8.53\text{--}8.67\text{ ppm}$), the ortho-ether linkage at high field ($7.05\text{--}7.3\text{ ppm}$) and the remaining aromatic hydrogen signals ($7.6\text{--}8.1\text{ ppm}$). The resemblance in the spectrum of SPPEK/silica indicates that the substitution similarly occurred at the σ -ether linkage sites of PPESK. According

to previous report,²³ the hydrogen atoms at the σ -ether linkage sites were more shielded than any other hydrogen atoms because of a resonance effect of the oxygens lone pair of electrons. Hence, in the upfield multiplet, there is upfield signals ($7.05\text{--}7.3\text{ ppm}$) arisen from the ortho to the ether linkage. Probably, it corresponds to H1/H4 of S or K phthalazinone units. A higher chemical shift upfield indicates that protons on this site would be most susceptible to sulfonation by electrophilic substitution.²¹

As shown in Figure 2(b), the ^1H spectrum of sulfonated PPESK shows a diminished upfield doublet, suggesting that sulfonation occurs at the position of H1/H4. Another characteristic of spectrum is the appearance of a series of downfield signals at $\delta 8.46$ as well as the disappearance of the multiplet at $\delta 8.67\text{--}8.53$. The changes in chemical shift indicate that the introduction of $-\text{SO}_3\text{H}$ group perturbs the downfield protons in the same aromatic ring.²¹

Dai *et al.*²¹ reported that H1/H4, meta to phthalazinone and ortho to the phenyl ether group, is the site where sulfonation is likely to occur most readily. The product of the sulfonation reaction is expected to occur at H1/H4 on SPPEK, as shown in Scheme I.

Morphology. Figure 3 shows SEM images of the SPPEK/silica membrane surface. Silica domains are observable. The average size of the silica domains is about $< 100\text{ nm}$.

The presence of the silica particles was confirmed using the energy-dispersive X-ray analysis (EDXA) attachment of FE-SEM. The hydrolysis of the TEOS added to the polymer solution led to the formation of a common network providing a good adhesion between organic and inorganic phases.

Thermal Analysis. TGA curves of the membranes are shown in Figure 4. The PPESK is thermally stable until 450°C , whereas the sulfonated PPESK membranes showed weight loss in several steps. Typically, thermal degradation of sulfonated polymer membranes can be divided into three

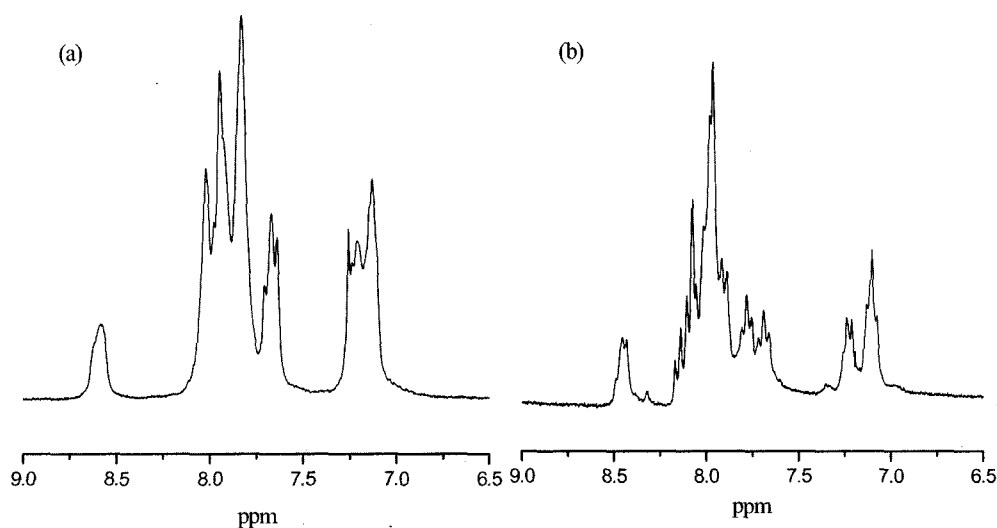
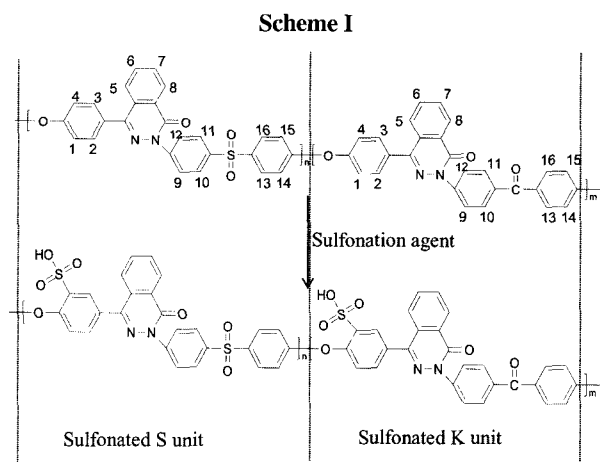


Figure 2. ^1H NMR spectrum of (a) PPESK and (b) sulfonated PPESK.



main degradation steps: Thermal solvation, thermal desulfonation and thermo-oxidation of a polymer matrix. The first weight loss at 100 °C was associated with the loss of absorbed water molecules. The absorbed water molecules in the membranes are supposed to exist in a bound state rather than in a free molecular state. The water molecule seems to be bound to the $-\text{SO}_3\text{H}$ due to hydrogen bonding. The second weight loss in the temperature range of $T = 250\text{--}400\text{ }^\circ\text{C}$ correspond to a loss of sulfonic acid by the desulfonation. In the third weight loss at temperature $> 450\text{ }^\circ\text{C}$, the polymer backbones were further degraded, corresponding to the decomposition of main chain of polymer. As shown in Figure 4(b), the weight residue of the HPS-Si hybrid membranes containing silica at 700 °C is higher than that of the HSP membrane and the 10% weight loss temperature of the HSP and HSP-Si membrane is about 373.6 and 396.3 °C, respectively. These results suggest that the introduction of silica into sulfonated PPESK membrane clearly enhances the thermal stability of hybrid materials.

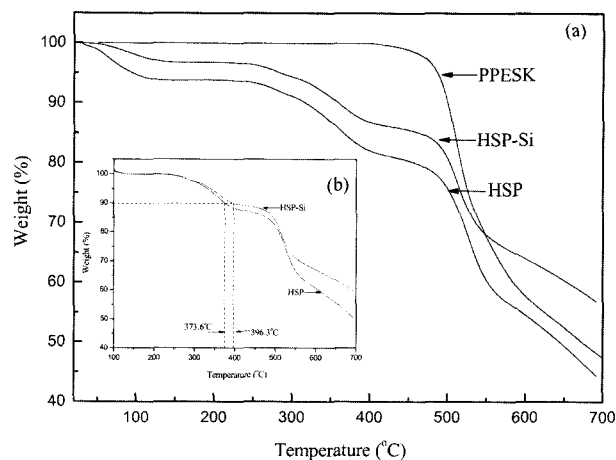


Figure 4. TGA curves of membranes.

Ion Exchange Capacity (IEC) and States of Water in Hybrid Membranes. IEC value of the membranes before and after boiling water test is summarized in Table I. The membranes possessed the IEC values in the range of 0.24–1.34 meq/g-dry membrane. The IEC values increased with the sulfonation time of PPESK due to the increasing charged ionic content ($-\text{SO}_3^-$) in membranes. The respective hydrolysis stability was evaluated using IEC value before and after boiling water test. As listed in Table I, IEC value did not change during the boiling water test.

The proton conductivity increases strongly with absorbed water content. Generally, the proton transport in the membrane occurs in two simultaneous mechanisms, namely, the Grotthuss mechanism and the vehicle mechanism. Proton transport in the Grotthuss mechanism involves a coordinated movement of the hydronium ion with the neighboring water molecules.³⁰ Therefore, it is important to know the state of water in the membrane.

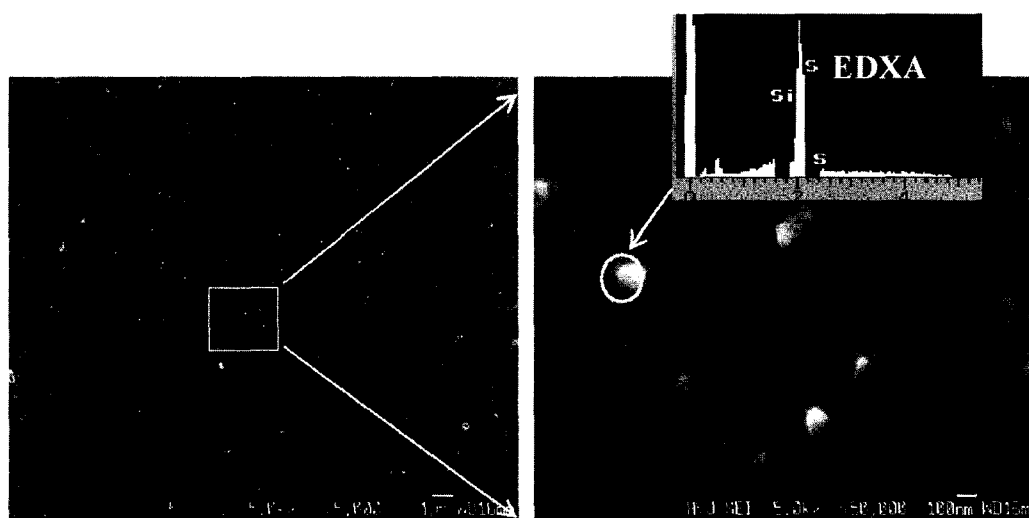


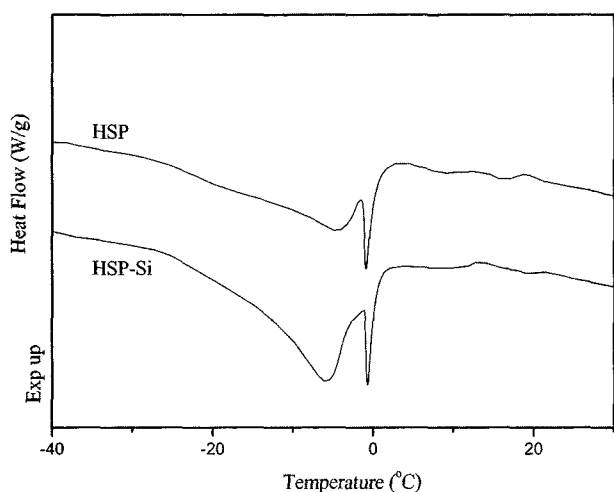
Figure 3. SEM image of sulfonated hybrid membrane surface (SP-Si 50).

Table I. Water Vapor Sorption (%), and IEC Value of SPPEsk after and before Boiling Water Test

Sample	Water Vapor Sorption (%)			IEC (meq./g)	
	RH 30	60	90	Before	After
SP-Si-6	1.6	2.3	4.8	0.28	0.27
SP-Si-10	2.1	2.9	5.7	0.34	0.34
SP-Si-20	2.5	3.5	6.8	0.4	0.4
SP-Si-30	3.4	5.0	9.2	0.56	0.55
SP-Si-50	7	10	18.5	0.96	0.96
HSP-Si	9.9	15.2	24.5	1.34	1.33
SP-6	1.4	2.3	4.6	0.3	0.29
SP-10	1.9	2.8	5.3	0.35	0.35
SP-20	2.5	3.3	6.4	0.41	0.40
SP-30	3.3	4.8	8.7	0.55	0.55
SP-50	6.5	9.1	17	1.1	1.1
HSP	9.5	14.5	23.8	1.34	1.33

In general, the states of water in a polymer can be distinguished into free water, freezing bound water and non-freezing bound water.³¹ Free water is defined as water that is not intimately bound to the polymer chain and has the same phase transition temperature as bulk water (0°C).³² Freezing bound water is defined as water that is weakly bound to the polymer chain or interacts weakly with non-freezing water and displays relatively broad melting endotherms. Non-freezing water is defined as water that has no detectable phase transition in temperature range -73 to 0°C, and arises from a strong interaction with the polymer.³²

Figure 5 shows the DSC curve of the water-swollen membrane, indicating that free water and freezing bound water exist in the membranes. Figure 6 exhibits the state of water

**Figure 5.** DSC melting curve of swelling membrane.

as a function of sulfonation time. The water content of membranes decreased in the order freezing bound water > free water > non-freezing bound water. However, in comparison with Nafion 117 membrane as listed in Table II, the HSP and HSP-Si membranes show higher non-freezing bound water than free water. This behavior may be attributed to the charged ionic content (-SO₃H) of the membrane and the morphological difference.³³ That is, the hydrogen bonding sites with water molecules of the HSP and HSP-Si membrane are higher than those of the Nafion membrane.

The proton conductivity of the membrane depends on their water content. In this study, the water vapor sorption was measured at different relative humidity (RH), since it is believed that these conditions resemble the conditions in a fuel cell.³⁴

The water vapor sorption (%) as a function of sulfonation time is listed in Table I. As listed in Table I, all of the hybrid membranes (SP-Si-XX) have somewhat higher water vapor sorption (%) as compared to unmodified SPPEsk membranes (SP-XX). This suggests that the number of ≡SiOH groups does increase the hydrophilicity of the membranes.

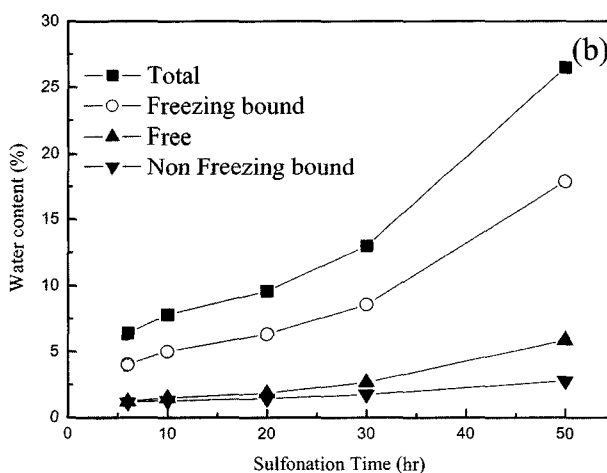
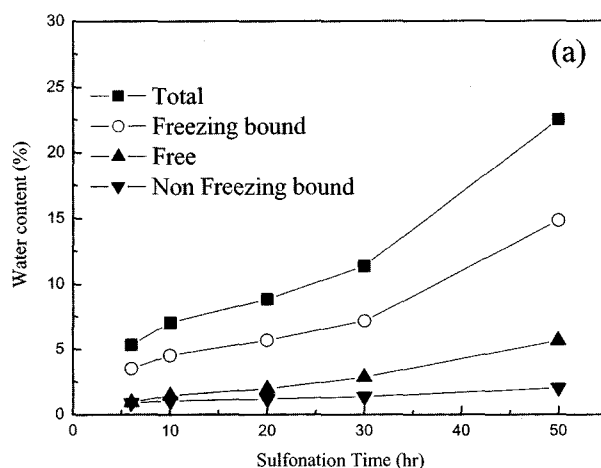
**Figure 6.** Composition of each state of water (a) SP-XX membranes (b) SP-Si-XX hybrid membranes.

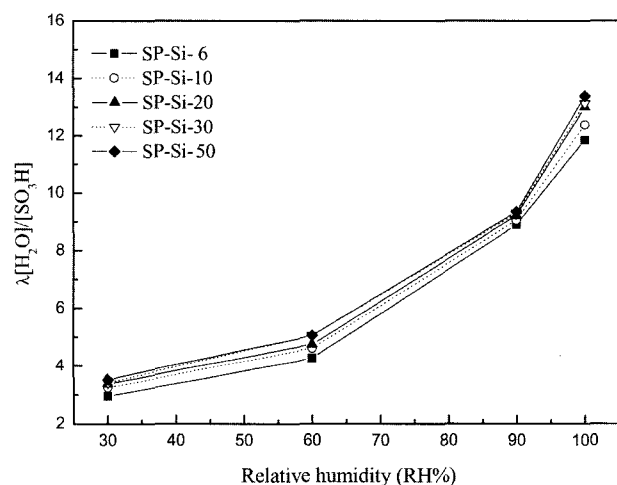
Table II. Characterization of Water Content, Composition of Each State of Water and Methanol Permeability of Highly Sulfonated PPESK and Nafion

Sample	Water Content (%)				λ [H ₂ O]/[SO ₃ H]				Methanol Permeability ($\times 10^{-7}$ cm ² /s)
	Total	Non-freezing Water ^a	Freezing Water ^b	Free Water ^c	Total	Non-freezing Water	Freezing Water	Free Water	
Nafion 117	26.5	3.0	17.4	6.1	16.4 (1) ^d	1.9 (0.11) ^e	10.7 (0.66) ^f	3.8 (0.23) ^g	23.6
HSP	40	9.8	24.2	6	16.6 (1)	4.1 (0.25)	10.0 (0.6)	2.5 (0.15)	6.6
HSP-Si	45	11.5	27	6.5	18.7 (1)	4.8 (0.26)	11.2 (0.6)	2.7 (0.14)	4.15

^aNon freezing bound water = $M_{total} - (M_{free} + M_{freezing\ bound})$. ^b $M_{free} = \Delta H_{free}/Q_{melting} \times M_{total}$ (total water).

^c $M_{freezing\ bound} = \Delta H_{freezing\ bound}/Q_{melting} \times M_{total}$ (ΔH : heat of melting of the water, $Q_{melting}$: the melting enthalpy of water at 0 °C, 334×10^3 J/kg).

^d[Total water, λ]/[Total water, λ]. ^e[Non-freezing water, λ]/[Total water, λ]. ^f[Freezing water, λ]/[Total water, λ]. ^g[Free water, λ]/[Total water, λ].

**Figure 7.** Number of water per sulfonic acid group of hybrid membranes (λ [H₂O]/[SO₃H]) as a function of RH (%).

The water vapor sorption behaviors as a function of the number of absorbed water molecules per sulfonic acid group (λ), vs. RH are shown in Figure 7. The λ and the water vapor sorption (%) increase with RH and IEC value.

As listed in Table II, the total λ of HSP and HSP-Si membrane are 16.6 and 18.7, respectively, which were higher than that of Nafion 117 (16.4). However, the fraction of freezing bound water and free water (characteristic of the ratio [freezing bound water, λ]/[total water, λ] and [free water, λ]/[total water, λ]) of HSP and HSP-Si membrane is lower than that of Nafion 117 membrane. In addition, the fraction of non-freezing bound water is a little higher for the HSP-Si hybrid membrane than for the HSP membrane. This effect was attributed to the presence of numerous \equiv SiOH groups to which H₂O molecules can hydrogen bond. Usually, perfluorinated polymer electrolytes show a decrease in conductivity with increasing temperature because of drying membrane, causing the channels for proton conductive to collapse, such that conductivity at 80 °C is decreased by more than 10 times relative to that at 60 °C.³⁵

Therefore, we expected that the proton conductivity of HSP and HSP-Si would maintain at higher temperature

because the HSP and HSP-Si membranes can reserve water content at high temperature by non-freezing and freezing bound water. We also expected that the proton conductivity of HSP-Si hybrid membrane was higher than that of the HSP membrane due to higher non-freezing bound water. This behavior will be discussed in the following section.

Proton Conductivity and Methanol Permeability. Generally, two principal mechanisms describe proton diffusion through membranes. The most trivial case of proton migration requires the translational dynamics of bigger species: this is the vehicle mechanism.³⁶ In this mechanism, proton combines with vehicles such as H₂O as H₃O⁺ and also unprotonated vehicles (H₂O) allows the net transport of protons. In the other principal mechanism, the protons are transferred from one vehicle to the other by hydrogen bonds. This mechanism is known as the Grotthuss mechanism.³⁶ In addition, Ren³⁰ reported that increasing the temperature diminishes the hydrogen bonding and consequently makes the proton jumping in the Grotthuss mechanism less successful. Therefore, it is said that the bound water participates in Grotthuss mechanism, and free water takes part in vehicle mechanism as well as Grotthuss mechanism. Therefore, the proton conducting membranes for use in high temperature required maintaining water content at high temperature, particularly the bound water.

The conductivity of the membranes with sulfonation time at 30 °C and RH 95% is shown in Figure 8(a). The proton conductivity increases with sulfonation time. In addition, the conductivity of hybrid membrane (SP-Si-XX) is higher than that of the membrane without silica (SP-XX). From this proton conductivity results, we suggest that the silica dispersed in membrane affect the forming the path way to transport proton due to the presence of numerous \equiv SiOH groups to which H₂O molecules can hydrogen bond. In comparison with the SP-XX membrane, the SP-Si-XX hybrid membranes show lower methanol permeability, that is, silica particle in the membrane acts as materials for blocking the methanol transport.

The proton conductivities of highly sulfonated membranes (HSP and HSP-Si) and Nafion 117 are shown in Figure 8 (b). The proton conductivity of the HSP and HSP-Si mem-

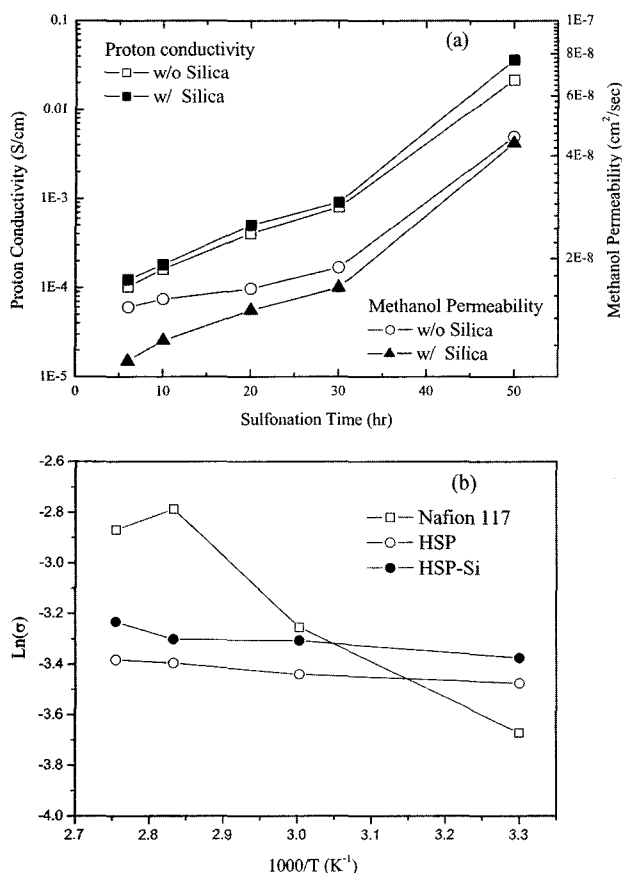


Figure 8. Proton conductivity and methanol permeability. (a) Effect of sulfonation time (RH 95%, 30°C) and (b) Arrhenius plot for proton conductivity for highly sulfonated PPESK (HSP, HSP-Si) and Nafion 117 (RH 95%) (The average estimated error was $\pm 5\%$).

brane is higher than that of Nafion 117 at low temperature due to high IEC value and water content. However, the increase of the proton conductivity with temperature is higher in Nafion 117 than in SPPEK and hybrid membranes. We supposed that the water content in the SPPEK and hybrid membrane likely did not increase with the increasing temperature at the vapor condition. This behavior may be attributed to the low acidity of the acidic functional group in SPPEK.

The conductivity of Nafion 117 increases up to 80°C and above this temperature it decreases. However, the HSP and HSP-Si membrane maintain the conductivity at 90°C. Especially, the conductivity of HSP-Si hybrid membrane increases at even 90°C. These results could be explained with number of water per sulfonic acid group (λ) as shown in Table II. The fraction of free water and freezing bound water of Nafion 117 is higher than that of HSP and HSP-Si membranes. The free water can act as a proton-carrying medium. However, the free water evaporates faster than bound water in a vaporized measuring condition with increasing temper-

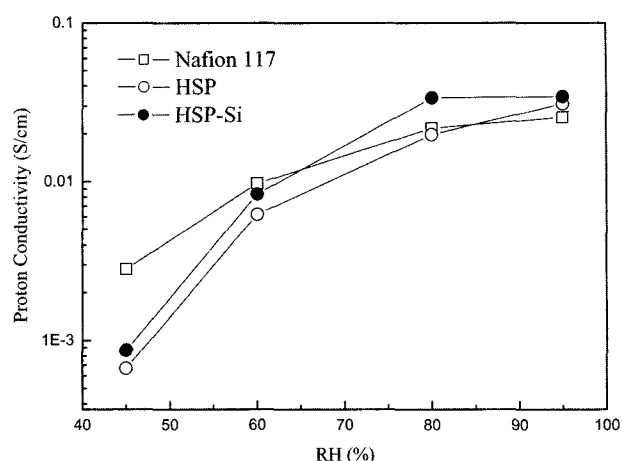


Figure 9. Proton conductivity of highly sulfonated PPESK (HSP, HSP-Si) and Nafion 117 at various relative humidity (RH %) at 30°C (The average estimated error was $\pm 5\%$).

ature. Therefore, in comparison with Nafion 117 membrane, the HSP and HSP-Si membranes could be maintained the water content at high temperature due to higher fraction of non-freezing bound water. Especially, the absorbed water by $\equiv\text{SiOH}$ in the HSP-Si hybrid membrane should be driven off around 170°C.²⁸ Therefore, the proton conductivity of the HSP-Si hybrid membrane increases at even 90°C.

Figure 9 shows the variation of proton conductive at 30°C with relative humidity (RH) for HSP, HSP-Si and Nafion 117 membrane. The proton conductivity increases with RH and this behavior tends similar to water vapor sorption (%). The conductivity increases by 1 to 2 orders of magnitude higher with increasing relative humidity from 30 to 95%.

Kim *et al.*³⁷ have reported that an important reason for the higher methanol permeability for Nafion is its higher fraction of freezing bound and free water as compared with that of the poly(arylene ether)-based copolymers. The same behavior was shown in our case. As summarized in Table II, Nafion 117 has undesirably high methanol permeability compared with that of HSP and HSP-Si hybrid membranes. The methanol permeability of the membranes decreased in the order Nafion 117 > HSP membrane > HSP-Si hybrid membrane. The fraction of free water of the Nafion 117, HSP and HSP-Si membrane decreased in the same order. Therefore, the free water would participate in methanol permeability. Note that Nafion 117 shows higher methanol permeability than that of sulfonated PPESK due to its higher fraction of free water.

Conclusions

The sulfonated poly(phthalazinone ether sulfone ketone) (SPPEK) and the sol-gel derived SPPEK/silica hybrid membranes were investigated as a potential polymer electrolyte for direct methanol fuel cell applications. In comparison

with membrane without silica, the hybrid membranes have a higher water content and improved proton conductivity as well as lower methanol permeability. In particular, the silica embedded in the membrane acted as a material for reducing the fraction of free water as well as a methanol barrier by reducing pathway to penetrate methanol molecules. The proton conductivities of SPPEK membranes were in the range of 10^{-3} and 10^{-2} S/cm and the methanol permeabilities were 10^{-8} and 10^{-7} cm²/sec. Note that the proton conductivity of HSP and HSP-Si membrane was not reduced at high temperature and these membranes show higher proton conductivity and lower methanol permeability than that of Nafion 117 at low temperature. From the results of proton conductivity and methanol permeability, it is suggested that the fraction of bound and free water should be optimized in order to obtain the desirable proton conductivity and methanol permeability. The SPPEK hybrid membrane having higher bound water and silica particles will be expected as a candidate as proton exchange membrane for DMFC. We will demonstrate the effect of silica content in the future.

Acknowledgements. This work was supported by the Korea Institute of Science and Technology Evaluation and Planning (KISTEP) under the National Research Laboratory Program and performed for the Carbon Dioxide Reduction & Sequestration Center, one of the 21st Century Frontier R&D Programs funded by the Ministry of Science and Technology of Korea.

References

- (1) X. Ren, M. S. Wilson, and S. Gottesfel, *J. Electrochem. Soc.*, **143**, 12 (1996).
- (2) N. A. Hampson, M. J. Wilars, and B. D. McNicol, *J. Power Sources*, **4**, 191 (1979).
- (3) A. Küver and W. Vielstich, *J. Power Sources*, **74**, 211 (1998).
- (4) S. P. Nunes, B. Ruffmann, E. Rikowski, S. Vetter, and K. Richau, *J. Membr. Sci.*, **203**, 215 (2002).
- (5) C. H. Brian, Steele, and H. Angelika, *Nature*, **414**, 345 (2001).
- (6) H. Dohle, *German Patent* 1980, 131C1 (1999).
- (7) R. P. Hamlen, *US Patent* 5849428 (1998).
- (8) J. Kjar, S. Yde-Andersen, N. A. Knudsen, and E. Skou, *Solid State Ionics*, **46**, 169 (1991).
- (9) Z. Plotarzewski, W. Wieczorek, J. Przymuski, and V. Antonucci, *Solid State Ionics*, **119**, 301 (1999).
- (10) P. L. Antonucci, A. S. Srico, P. Creti, E. Ramunni, and V. Antonucci, *Solid State Ionics*, **125**, 431 (1999).
- (11) K. A. Mauritz, I. D. Stefanithis, S. V. Davis, R. W. Scheetz, R. K. pope, and G. L. Wilkes, *J. Appl. Polym. Sci.*, **55**, 181 (1995).
- (12) A. Bunn and J. B. Rose, *Polymer*, **34**, 1114 (1993).
- (13) M. Ueda, H. Toyota, T. Ouchi, J. I. Sugiyama, K. Yonetake, T. Masuko, and T. Teramoyo, *J. Polym. Sci.; Part A: Polym. Chem.*, **31**, 853 (1993).
- (14) H. S. Chao, N. Y. Watervliet, D. S. Kelsey, and N. J. Hillsborough, *US Patent* 4,625,000 (1986).
- (15) A. Noshay and L. M. Robeson, *J. Appl. Polym. Sci.*, **20**, 1885 (1976).
- (16) S. Holmberg, J. Nasman, and F. Sundholm, *Polym. Adv. Technol.*, **9**(2), 121 (1998).
- (17) J. Kerres, W. Cui, and S. Reichle, *J. Polym. Sci.*, **34**, 2421 (1996).
- (18) R. Nolte, K. Ledjeff, M. Bauer, and R. Mülhaupt, *J. Membr. Sci.*, **83**, 211 (1993).
- (19) S. M. J. Zaidi, S. D. Mikhailenko, G. P. Robertson, M. D. Guiver, and S. Kaliaguine, *J. Membr. Sci.*, **173**, 17 (2000).
- (20) S. Koter, P. Piotrowski, and J. Kerres, *J. Membr. Sci.*, **153**, 83 (1999).
- (21) Y. Dai, X. Jian, X. Liu, and M. D. Guiver, *J. Appl. Polym. Sci.*, **79**, 1685 (2001).
- (22) G. Xiao, G. Sun, D. Yan, P. Ahu, and P. Tao, *Polymer*, **43**, 5335 (2002).
- (23) Y. Gao, G. P. Robertson, M. D. Guiver, and X. Jian, *J. Polym. Sci., Part A*, **41**, 497 (2003).
- (24) Y. Gao, G. P. Robertson, M. D. Guiver, X. Jian, and S. D. Mikhailenko, *J. Polym. Sci., Part A*, **41**, 2731 (2003).
- (25) Y. Gao, G. P. Robertson, M. D. Guiver, X. Jian, S. D. Mikhailenko, K. Wang, and S. Kaliaguine, *J. Membr. Sci.*, **227**, 39 (2003).
- (26) N. Carretta, V. Tricoli, and F. Picchioni, *J. Membr. Sci.*, **166**, 189 (2000).
- (27) F. Wang, T. Chen, and J. Xu, *Macromol. Chem. Phys.*, **199**, 1421 (1998).
- (28) Q. Deng, R. B. Moore, and K. A. Mauritz, *J. Appl. Polym. Sci.*, **68**, 747 (1998).
- (29) N. Miyake, J. S. Wainright, and R. F. Savinell, *J. Electrochem. Soc.*, **148**, A898 (2001).
- (30) X. Ren and S. Gottesfeld, *J. Electrochem. Soc.*, **148**, A87 (2001).
- (31) P. Samuel, Kusumocahyo, S. Kenji, S. Masao, and K. Mizoguchi, *Separ. & Puri. Techn.*, **18**, 141, (2000).
- (32) A. Higuchi and T. Iijima, *Polymer*, **26**, 1207 (1985).
- (33) K. D. Kreuer, *J. Membr. Sci.*, **185**, 29 (2001)
- (34) S. Hietala, S. L. Maunu, F. Sundholm, T. Lehtinen, and G. Sundholm, *J. Polym. Sci., Part B*, **37**, 2893 (1999).
- (35) M. Rikukawa and K. Sanui, *Prog. Polym. Sci.*, **25**, 1463 (2000).
- (36) K. D. Kreuer, *Chem. Mater.*, **8**, 610 (1996).
- (37) Y. S. Kim, L. Dong, M. A. Hickner, T. E. Glass, V. Webb, and J. E. McGrath, *Macromolecules*, **36**(17), 6281 (2003).